JOURNAL OF APPLIED ELECTROCHEMISTRY 23 (1993) 781–789

Anodic formation of polypyrrole/tungsten trioxide composites

F. BECK, M. DAHLHAUS

Fachgebiet Elektrochemie, University of Duisburg, Lotharstrasse 1, D-4100 Duisburg 1, Germany

Received 3 July 1992; revised 25 October 1992

The anodic codeposition of WO_3 and polypyrrole at constant current densities was studied. The powdery solid was dispersed in the electrolyte (0.1 M pyrrole, 0.1 M $LiClO_4$) under strong convection at $c_E = 0.01$–$30\,g\,dm^{-3}$. Water or wet acetonitrile were employed as solvents. Various modes of convection were developed. The resulting WO_3 concentrations in the PPy/WO_3 composites were up to $c_C = 53\,wt\,\%$. c_C was found to increase with increasing convection intensity and with decreasing current density. Quantitative evaluation leads to a relationship $c_C = K \log c_E/c_{E,0}$, where K is a constant and $c_{E,0}$ is a threshold concentration. This equation was derived from a model assuming a Temkin type adsorption of the impinging particles and their field enhanced final incorporation into the polypyrrole matrix. K is proportional to j^{-1}. The new model complements the older theory of Guglielmi, originally developed for systems with metal matrices, and it also holds for these very well known composites. The homogeneous distribution of WO_3 in PPy is demonstrated by the linear increase of the WO_3 mass with the thickness of the composite in combination with SEM techniques.

1. Introduction

Cathodic codeposition of metals and finely dispersed materials under strong convection is a well established technique for the manufacture of composites [1–21]. Initial work reaches back about forty years, where the galvanic formation of a Ni/diamond dust composite for a tool was claimed in a patent [1]. Common features of the new materials are a uniform distribution of the particles in the metal matrix and the utilization of standard bath compositions. Up to now, a considerable amount of experience has accumulated in this field. In most cases, nickel as a matrix is used. The dispersed materials are oxides such as Al_2O_3 [2–7] or TiO_2 [8, 9]. In addition, non oxide hard materials such as SiC [9–11] or Si_3N_4 [12] were successfully incorporated. Graphite powder was dispersed in copper [10], and diamond dust in nickel [1, 13]. Inorganic systems such as ZnS [14], Nb_3GeAl [15], NiAl [16] or $LaNiO_3$ [17] were dispersed in a metal matrix as a manufacturing step for increasing wear resistance, in the manufacture of superconducting cables and for electrohydrogenation or hydrogen evolution catalysts, respectively. It is also possible to codeposit dispersed polymers such as phenol resin powders into zinc [18] or coloured acrylate dispersions into nickel [19]. The whole field is covered in two useful review articles [20, 21].

More recently this method has been used for the anodic codeposition of synthetic metals such as polypyrrole and dispersed solids. Yoneyama and coworkers were the first to achieve the anodic formation of PPy/TiO_2 composites in non-stirred organic solutions in the absence of a supporting electrolyte [22, 23]. The transport of the dispersed material was due to electrophoresis. The same strategy was employed for colloidal Prussian blue [24] and for elastomeric latices [25]. However, this interesting method leads to a relatively low concentration in the solid. Electrodeposition of PPy/TiO_2-composites from heterogeneous, strongly stirred electrolytes, in analogy to [1–21], were reported independently by a Japanese [26] and a German [27] group. Strong convection was an essential feature. It was found that the rate of codeposition was appreciably higher than in Yoneyama's case, and that the levels of pigment concentrations exceeded even those commonly found with metals [27]. This was attributed to a relatively rough surface at the growing polymer layer. It should be pointed out, that this is the only way to fabricate composite materials with a matrix of unfusable and insoluble synthetic metals. The opposite case – conventional polymers as the matrix and powdery synthetic metals as fillers – has frequently been reported in the past, and some characteristic examples are compiled in [27].

In the following, a detailed investigation into the system PPy/WO_3 is reported. WO_3 is a heavy pigment ($s = 7.16\,g\,cm^{-3}$) with interesting photoelectrochemical properties. The anodic codeposition is discussed in this paper, while the characterization of the novel material will be treated in a subsequent publication [28].

2. Experimental details

The temperature was 20 °C throughout. All electrolytes were deaerated by bubbling with argon.

Two kinds of base electrodes were employed: (1) cylindrical Pt-electrodes, 1 mm diam., $A = 0.5\,cm^2$

0021-891X

for electrochemical measurements, and (2) sheet electrodes, made from 0.1 mm smooth Pt or 1 mm polished stainless steel, $A = 30\,cm^2$ ($2 \times 2.5\,cm \times 6\,cm$) exposed area, both sides, were used for preparative codepositions.

Pyrrole (Merck, zur Synthese) was freshly distilled at 1 bar under nitrogen. Acetonitrile (Merck, zur Synthese) was used as received, the water concentration was adjusted to 0.1 M. $LiClO_4$ (Merck, analytical grade) was used directly. WO_3 (Merck, reinst) was used as received. The medium particle sizes were measured with the help of a SALD-1100 laser diffractive particle size analyser (Shimadzu) to be 10 μm. Further treatment in a ball mill led to agglomeration. Electrodeposition was performed galvanostatically under two different conditions at pyrrole concentrations of 0.1 M:

(I) 0.1 M $LiClO_4$, 0.1 M H_2O in MeCN, $j = 0.5\,mA\,cm^{-2}$ (Diaz conditions [29])
(II) 0.1 M $LiClO_4$ in H_2O, $j = 2\,mA\,cm^{-2}$ (aqueous electrolyte)

The electrolyte/dispersoid system was replaced by a fresh one after each preparative codeposition.

The nominal thickness d_n of the coating was 10 μm. d_n was calculated with the assumption of 100% current efficiency, a density of $1.5\,g\,cm^{-3}$ and a degree of insertion of $y = 33\%$ [30]. This led to a deposition time at $2\,mA\,cm^{-2}$ for $d_n = 10\,\mu m$ of exactly 30 min.

The cylindrical glass cells had a typical capacity of 250 ml. Strong forced convection was produced in four ways:

(I) Rotation of the sheet anode around the longer line of symmetry [27]. The rotation speed was 50 r.p.m. A magnetic stirrer rotated in the opposite direction at 300 r.p.m. This relatively strong mode is termed 'RE' in the following.
(II) Pumping of the suspension in a loop, *cf.* Fig. 1 in [27]. The flow rate was up to $25\,ml\,s^{-1}$. This mode of convection is symbolized as 'PL'.
(III) Ultrasonic stirring ('US'). The cell was located in an aqueous ultrasonic bath (Bransonic 52). The inner electrolyte level and the external water level were identical.
(IV) According to Fig. 1 an intensive stirrer [31] with 10 stainless steel blades was arranged in about 1 cm distance in front of the anode ('IS'). This mode of convection was the best. Only one side of the anode was coated, the other side was tightly covered by a PTFE holder with natural caoutchouc sealings.

In modes (I)–(III) two counter electrodes were used, in (IV) only one; these were of stainless steel. The reference electrode was a NaCl saturated calomel electrode, which is +236 mV positive to SHE. The potentials against this reference are denoted as U_{SSCE}.

After electrodeposition, the electrodes were thoroughly rinsed with the solvent and dried in vacuo.

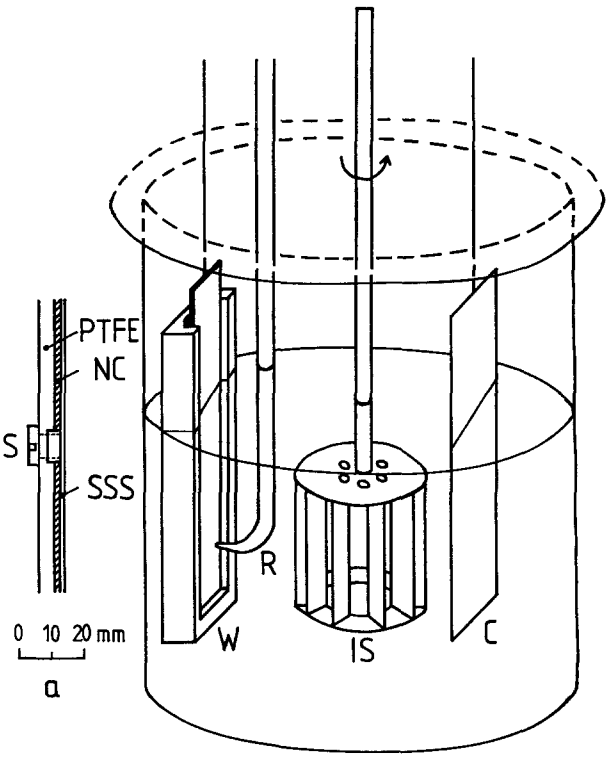

Fig. 1. Cell with an intensive stirrer IS for codeposition of PPy and dispersed WO_3 under strong convection mode IS. W: working electrode, C: counter electrode, (a) details of W (side view): PTFE: holder, machined from PTFE, NC: natural caoutchouc, SSS: stainless steel sheet, S: screw. The cover of the glass cell is not shown.

The WO_3 concentration was determined as follows. The loaded polypyrrole film was oxidized in 2 ml hot concentrated HNO_3 (68%) in a small glass beaker to destroy the organic material. After evaporation of the acid almost to dryness, the residue was fumed off with 2 ml concentrated H_2SO_4. The material was then dissolved in 5 ml 2 M NaOH. Thereafter, 10 ml 5 M NH_4SCN, 10 ml 20% HCl and 10 ml 15% $TiCl_3$ in 20% HCl were added. After dilution to 50 ml with distilled H_2O, the yellow W-V-complex $H[W(OH)_2(SCN)_4]$ was photometrically determined at 406 nm [32].

3. Results

3.1. *General remarks*

The results on the PPy/WO_3-system are presented in two groups. The electrodeposition is reported in the present paper. The characterization of the novel composites is devoted to a separate paper [28]. Table 1 shows the nomenclature used for the mode of convection and the electrolytes used.

Table 1. Symbols for electrolytes and convection modes

Convection mode	*Electrolyte I (MeCN, Diaz)*	*Electrolyte II (H_2O)*
US (3)	+	★
RE (1)	△	▲
PL (2)	○	●
IS (4)	□	■

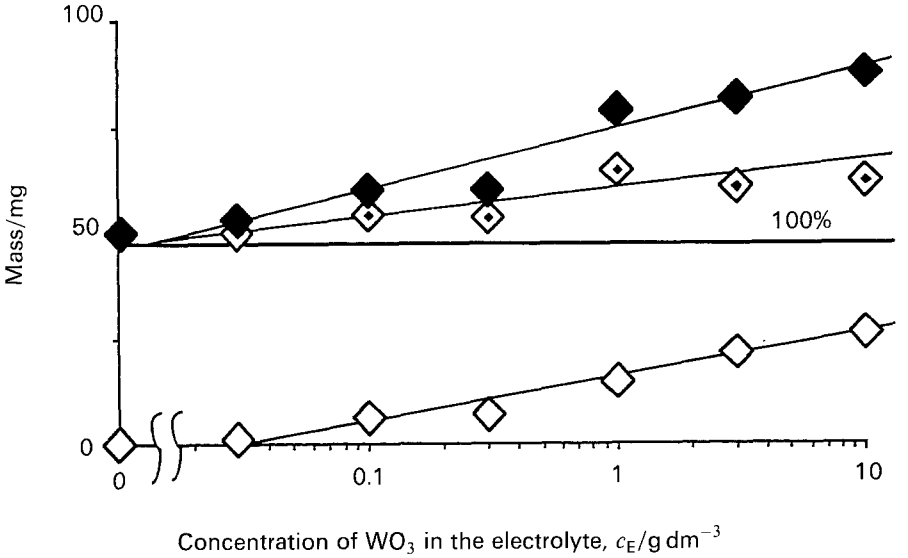

Fig. 2. Plot of mass m of electrodeposited materials against logarithm of c_E. Electrolyte I (MeCN), $j = 0.5\,mA\,cm^{-2}$, $d_n = 10\,\mu m$, convection mode PL. (◆) total mass, (◇) mass of polypyrrole, (◇) mass of WO_3. (————) line for 100% c.e., blank PPy.

3.2. *Potential–time curves*

The anodic deposition experiments were performed under galvanostatic conditions. At platinum as a substrate, the potential–time curves are relatively featureless and the potential is constant, as also found for pigment free electrolytes [30]. However, in the case of stainless steel, which is the preferred anode material on practical grounds, an initial potential peak is observed, which may be due to hindered nucleation of polypyrrole at the mixed oxide surface. After about 10 s, the two curves coincide.

At more extended times a slow negative potential shift is generally observed. The reason for this must be an increasing surface roughness. This effect is initially further enhanced with increasing pigment concentration, c_E, in the electrolyte. Interestingly, at the highest c_E the difference decreases. This effect may be caused through an increased surface coverage by the oxide particles, which shield part of the surface of the growing polypyrrole layer.

3.3. *Variation of WO_3-concentration in the electrolyte c_E*

Figure 2 displays the mass of the composite, m_{total}, and the analytically determined mass of WO_3, m_{WO_3} as a function of $\log c_E$. The mass of polypyrrole binder $m_{PPy'}$ is:

$$m_{PPy} = m_{total} - m_{WO_3} \quad (1)$$

Figure 2 shows that m_{WO_3} rises, after an induction period, in proportion to the logarithm of c_E. Almost 100% current efficiency ($m_{PPy,th} = 47\,mg$) is found for the composites from electrolyte I, *cf.* Section 3.6.

Figure 3 shows a semilogarithmic plot of the two concentrations, c_E and c_C, in electrolyte I (MeCN). Clearly, c_C rises logarithmically with c_E, starting from a threshold concentration $c_{E,0'}$ which is between 0.1 and 0.01 g dm^{-3}. A pronounced influence of the convection mode can be recognized. The slope of the lines increases with increasing convection intensity. Interestingly, it was observed with the 'IS' cell,

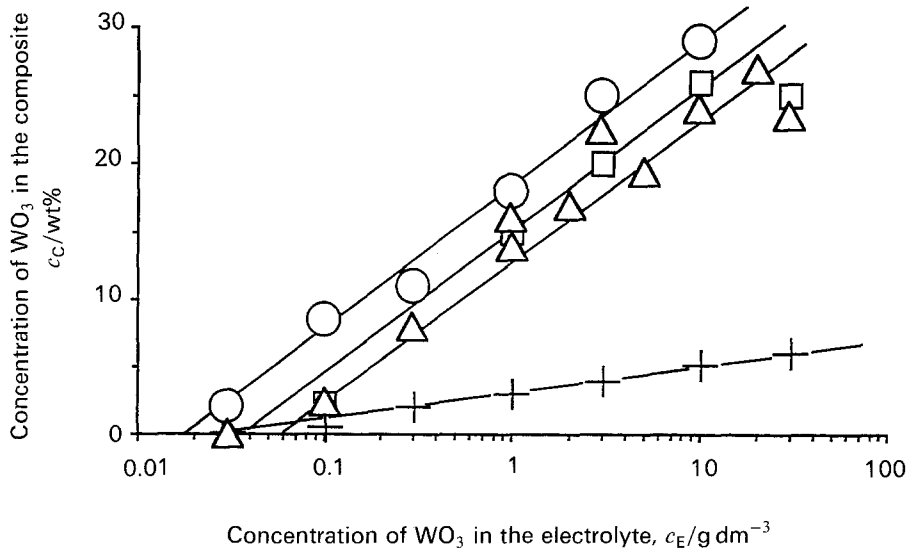

Fig. 3. $c_C/\log c_E$-plots for anodic formation of PPy/WO_3 codeposits from electrolyte I (*MeCN*) at four different convection modes according to Table 1. $j = 0.5\,mA\,cm^{-2}$, $d_n = 10\,\mu m$.

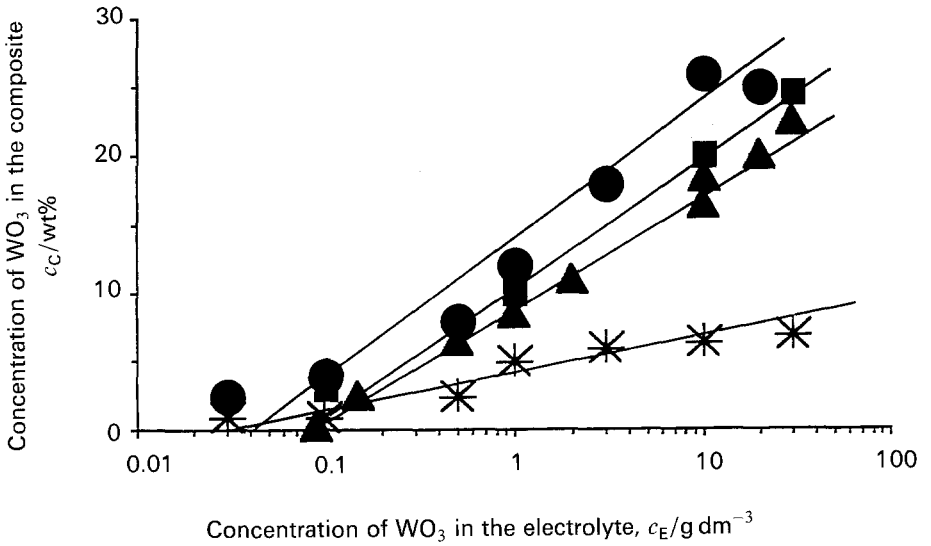

Fig. 4. The same as Fig. 3, but with the *aqueous* electrolyte II. $j = 2\,\text{mA cm}^{-2}$, $d_n = 10\,\mu\text{m}$.

that a very high intensity of convection led to a decrease in c_C at constant c_E. A weak tendency towards saturation can be seen at the highest c_E's.

Nearly identical features are found for the aqueous electrolyte II, *cf.* Fig. 4. At constant c_E, the c_C values in the case of I are somewhat higher than for the system II ($\Delta c_C \approx 5\%$), at least for the steeper lines. These results clearly demonstrate that it is possible to control c_C over a wide interval by a selection of appropriate electrolyte concentrations of the dispersoid (c_E).

3.4. *Variation of thickness d_n of the deposit*

As well as the standard thickness, $d_n = 10\,\mu\text{m}$, some other composite foils with thicknesses between 3 and 40 μm were manufactured. Two examples with the aqueous systems II are shown in Fig. 5. Clearly, the two masses, m_{total} and m_{WO_3}, which can be determined experimentally, increase in proportion to d_n. This is also the case for the polypyrrole mass given by Equation 1. m_{total} is a little high, if the electrolyte is not removed completely from the pores of the composite. However, in contrast to previous results with blank polypyrrole [29], the difference between thorough rinsing with the solvent and 30 min leaching in boiling acetonitrile was relatively small, as shown in Table 2. Boiling with methanol was omitted due to the reactivity of WO_3. The WO_3 masses(†) were determined analytically. This, after treatment, was normally confined to method (II). Thus the values for m_{PPy} and therefore for γ (Tables 3 and 4) are somewhat high, *cf.* Fig. 5.

3.5. *Variation of current density j*

It is assumed that the incorporation of the impinging particles itself is a rate process. A decrease of c_C with increasing j must be observed, where the current density is responsible for the growth of thickness of the PPy-matrix. Indeed the highest c_C occurs at the lowest current densities. A plot of c_C against $1/j$ is given in Fig. 6. A hyperbolic function is found over a range of current densities, but with a finite value for c_C at high c.d.s. This will be discussed further in Section 4.

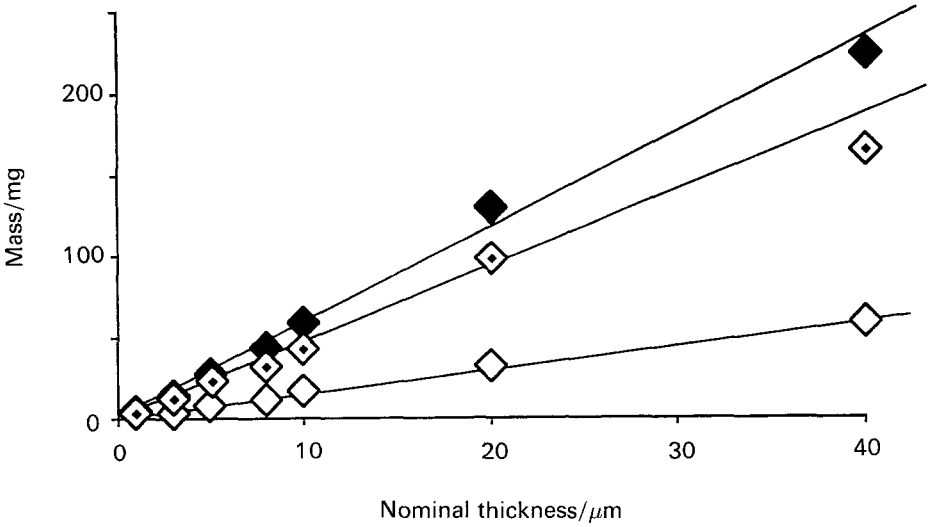

Fig. 5. Plot of mass m of electrodeposited materials against nominal thickness d_n Electrolyte II (H_2O), $j = 2\,\text{mA cm}^{-2}$, convection mode PL. (◆) total mass, (◈) mass of polypyrrole, (◇) mass of WO_3.

Table 2. Effect of electrode treatment after electrodeposition. Standard thickness 10 μm, $A = 30\,cm^2$, $c_E = 10\,g\,dm^{-3}$, *electrolyte I, convection RE*

	m_{PPy}/mg
(I) Theoretical value	47
(II) Thorough rinsing with the solvent	70.4* − 15.3† = 55.1
(III) Leaching 30 min in boiling MeCN	67.4* − 17.5† = 49.9

* m_{tot}; † m_{WO_3}

3.6. *Current efficiency γ for PPy-formation*

The polypyrrole mass m_{PPy} can be easily determined from Equation 1. From this, the current efficiency γ for the electrodeposition of PPy in the presence of finely dispersed WO_3 can be calculated according to

$$\gamma = \frac{m_{PPy}}{m_{th}} = \frac{m_{PPy}F(2+y)}{(M+yM_A)Q} \qquad (2)$$

where M is the molar mass of a PPy monomer unit ($M = 65$), M_A is the molar mass of the anion, y its degree of insertion and Q is the charge passed. Table 3 compiles some data, where y was assumed to have an average value of 0.33.

It can be seen that γ is generally high. It ranges from 90 to 121%, and is almost unaffected by the presence of WO_3. The values above 100% may be attributed to some retention of electrolyte components in the polymer exceeding normal doping. It should be pointed out that the boiling of the product in methanol was omitted. But this is necessary to remove *all* the electrolyte components from the pores.

An attempt was made to employ the bromide catalysed MeCN-electrolyte in order to accelerate the rate of electrodeposition [33, 34]. The electrolyte composition was:

III MeCN, 0.1 M pyrrole, 0.1 M NBu_4BF_4,
1 mM NBu_4Br, 0.03 M H_2O

Table 4 gives some results for this system. It can be seen that the current efficiencies are appreciably lower, especially under strong convection, which is needed for the codeposition of the particles. This is due to the negative stirring effect [34]. Interestingly, relatively high current efficiencies were found for the composites. The highest WO_3-concentrations were obtained under these conditions.

3.7. *WO_3-reduction at the counter electrode*

The codepositions were performed in undivided cells. At least for aqueous systems, a reduction of WO_3 to pentavalent or tetravalent oxide moieties seems to be possible. The corresponding redox potentials are both − 0.27 V/SCE. Adhering WO_x layers at the cathode exhibited a blue–green colour. Voltammetric curves measured in the negative direction in the presence of $10\,g\,dm^{-3}$ WO_3 dispersed in moist $MeCN/LiClO_4$ electrolyte give two cathodic waves at − 0.1 and − 0.75 V, which are not present in the blank electrolyte. Continuous electrodepositions in undivided cells may become problematic due to the accumulation of partially reduced WO_3. Another critical point is the acid/base balance in the cell, and slight acidification may lead to the chemical formation of pyrrole oligomers [35]. As mentioned in the experimental section, the electrolyte was renewed after each preparative run.

4. Discussion

It was found that the incorporation of dispersed TiO_2 [27] or WO_3 in anodically growing polypyrrole layers is possible under strong convection. This is the only way to manufacture such composite materials. The concentration, c_C of the fillers in the composite are distinctly influenced by their concentration in

Table 3. Current efficiencies γ for PPy, calculated after Equations 1 + 2. $y = 0.33$, $Q = 108$ C (54 C): $d_n = 10\,\mu m$.

Electrode	$c_E/g\,dm^{-3}$	*Convection*	m_{tot}/mg	m_{WO_3}/mg	m_{PPy}/mg *(after Eqn. 1)*	$\gamma/\%$ *(after Eqn. 2)*
I	0	US	54.6	0.0	54.6	116
I	0	RE	56.0	0.0	56.0	119
I	0	PL	56.8	0.0	56.8	121
I	0	IS	26.0*	0.0	52.0	110
I	10	US	58.1	2.8	55.3	117
I	10	RE	70.4	15.3	55.1	117
I	10	PL	74.5	19.4	55.1	117
I	10	IS	34.4*	8.8*	25.6	109
II	0	US	49.4	0.0	49.4	105
II	0	RE	44.7	0.0	44.7	95
II	0	PL	46.6	0.0	46.6	99
II	0	IS	24.9*	0.0	49.8	106
II	10	US	48.6	2.8	45.8	97
II	10	RE	55.2	10.2	45.0	96
II	10	PL	59.5	16.9	42.6	90
II	10	IS	29.3*	7.2*	22.1	94

* Coating of only one side.

Table 4. Current efficiencies for bromide catalysed electrodeposition of PPy, $Q = 108\,C$, $d_n = 10\,\mu m$, $m_{PPy,th} = 47\,mg$ (Electrolyte III)

$c_E/g\,dm^{-3}$	*Convection (RE)*	m_{tot}/mg	m_{WO_3}/mg	m_{PPy}/mg *(after Eqn. 1)*	$c_C/wt\,\%$	$\gamma/\%$ *(after Eqn. 2)*
0	weak	40	–	40	–	85
0	medium	33	–	33	–	70
0	strong	29	–	29	–	62
2	medium	71	26.4	44.6	37	95
5	medium	82	28.7	40.2	35	85
10	medium	95.5	51.0	44.5	53	95
20	medium	94	49.8	44.2	53	94

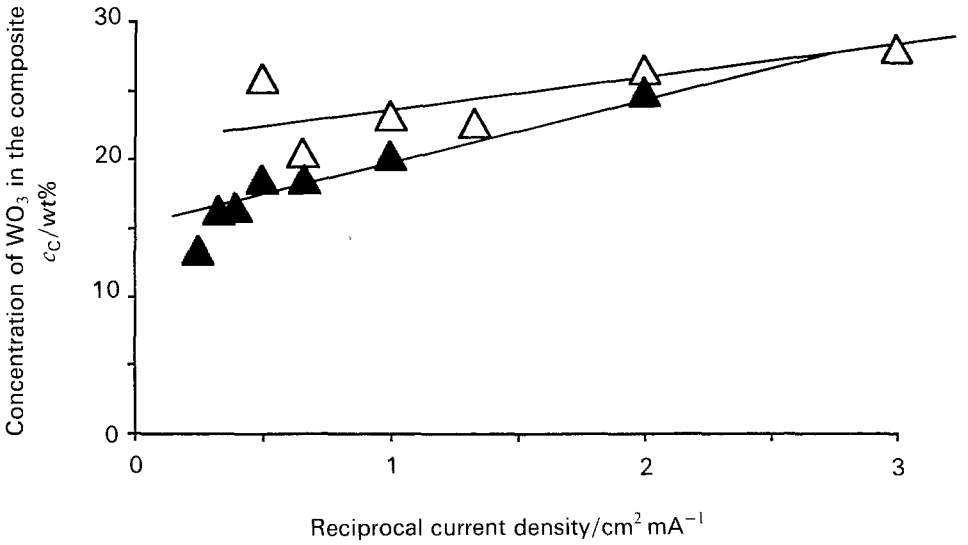

Fig. 6. Influence of current density j. A plot of c_C against the inverse of j. $d_n = 10\,\mu m$, $c_E = 10\,g\,WO_3\,dm^{-3}$. (△) Electrolyte I (MeCN), $j = 0.5\,mA\,cm^{-2}$, (▲) Electrolyte II (H_2O), $j = 2\,mA\,cm^{-2}$. Convection mode: RE.

the electrolyte, c_E, and the intensity of convection. When compared to the well known codeposits metal/filler, c_C in terms of wt % is higher by a factor of 2–10. This is demonstrated with two examples for each group in Fig. 7. Differences are smaller if concentrations are expressed in vol %, *cf.* [27]. These effects are partially caused by the differences in the density of the matrix and/or filler. Ni/PPy yields a ratio of 5.5, and WO_3/TiO_2 a ratio of 1.7. But another important feature is the softer and rougher surface of the polypyrrole, as pointed out in [27].

Figures 3, 4 and 7 show clearly that a logarithmic law holds for the c_C/c_E relationship. The only theoretical treatment presently available for metal composites is that of Guglielmi [8]. On the basis of a model, where the particles are 'adsorbed' according to a Langmuir type isotherm, and then are incorporated in a second, field enhanced, rate process, the following equation is derived:

$$\frac{c_E}{c_C} = K_1 + K_2 c_E \tag{3}$$

where K_1 and K_2 are constants. The validity of this relationship for PPy/TiO_2 composites was already shown [27].

On the other hand, the present logarithmic law indicated by the experimental results suggests that

$$c_C = K \log \frac{c_E}{c_{E,0}} \tag{4}$$

where K is a constant and $c_{E,0}$ is a threshold concentration. Equation 4 can be derived from first principles from a mechanism, which is similar to that of Guglielmi. If convection is intensive enough, a strong interaction, not only between the particles and the surface, but also between the particles themselves in the free, as well as adsorbed state, occurs. The latter kind of interaction is a negative (repulsive) one. It increases with c_E, and finally the incorporation step is strongly retarded. Such behaviour is described on a molecular scale by the Frumkin and the logarithmic Temkin adsorption isotherms. For the present particle system the individual steps are identical to the molecular events. Then the concentration of adsorbed particles is given by

$$c_{ad} = \kappa \log \frac{c_E}{c_{E,0}} \tag{5}$$

where κ is a constant.

The rate of particle incorporation into the composite is defined in the same way as in Gugliemi's work to be a field enhanced process:

$$\frac{dm_{WO_3}}{dt} = \kappa_1 c_{ad} \exp(B\Delta\varphi) \tag{6}$$

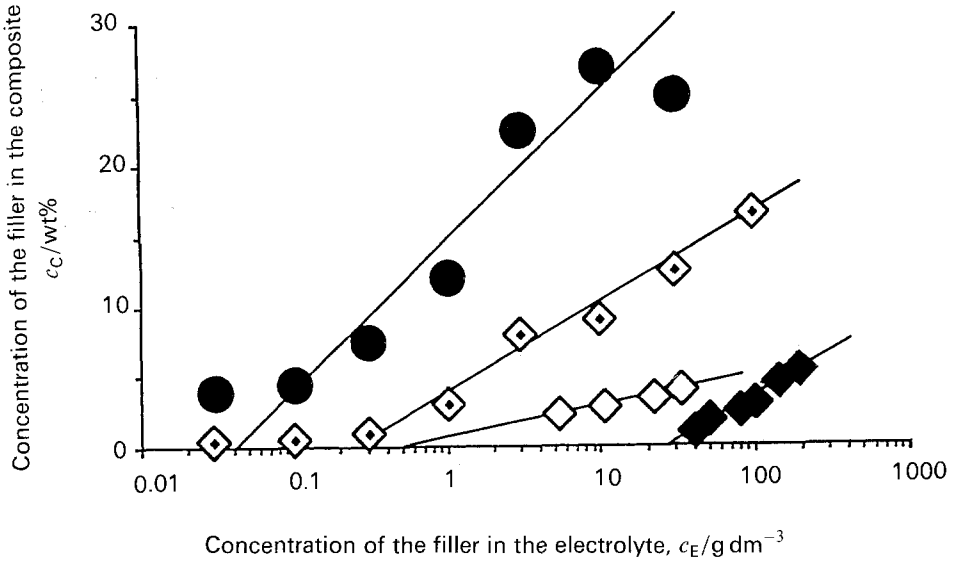

Fig. 7. Comparative plots c_C against log c_E for two PPy- and two Ni-composites, convection mode PL. (●) PPy/WO_3, electrolyte II (H_2O), PL, 10 μm; (◈) PPy/TiO_2, electrolyte II (H_2O), PL, 10 μm, from [27]; (◇) Ni/TiO_2, from [8], aqueous bath (20 mA cm^{-2}); and (◆) Ni/SiC, from [11], aqueous bath (100 mA cm^{-2}).

κ_1 and B are further constants, and $\Delta\varphi$ is the Galvani voltage, which contains the overvoltage η as a term of a sum, *cf.* Equation 10.

The rate of electrodeposition of polypyrrole is given by Faraday's law:

$$\frac{dm_{PPy}}{dt} = \frac{\gamma M_{eff} A}{zF} j \tag{7}$$

where γ is the current efficiency, A the surface area and j the current density. $M_{eff} = M + yM_A$ and $z = 2 + y$ are defined according to Equation 2. The pigment concentration in the composite (in wt%) is given by

$$c_C = \frac{\left(\frac{dm_{WO_3}}{dt}\right)}{\left(\frac{dm_{PPy}}{dt}\right) + \left(\frac{dm_{WO_3}}{dt}\right)} \tag{8}$$

For small loadings, the second term in the denominator can be neglected. Substituting Equations 5–7 into Equation 8 leads to:

$$c_C = \frac{z\kappa\kappa_1 F \exp(B\Delta\varphi)}{\gamma M_{eff} jA} \log \frac{c_E}{c_{E,0}} \tag{9}$$

At constant current density the prelogarithmic term becomes constant, and it is identical with K in Equation 4. The convection effect may be governed via κ, which increases with increasing kinetic energy of the impinging particles. This holds especially for soft and rough surfaces, as in the case of polymer matrices.

A negative effect of convection rate may become important at very high intensities due to 'shooting away' of particles, which reside at the surface. The tendency to saturation of c_C at high c_E may be explained accordingly, together with the fact that the simplification of Equation 8 becomes invalid.

The influence of the current density should be a hyperbolic one, according to Equation 9. This is confirmed, *cf.* Fig. 6. However, c_C does not approach zero at high js, but it reaches a limiting value. This can be understood in terms of a partial compensation due to an increase of the exponential factor at high current densities, which leads to high overvoltages η:

$$\Delta\varphi = \Delta\varphi_0 + \eta \tag{10}$$

The results in Fig. 5, according to which the masses for WO_3 and PPy, and thus the total mass, increase with the thickness d_n prove the homogeneous distribution of the pigment in the composite. However, this proof is not at all an unequivocal one. The measured increase in surface roughness with increasing d_n [36], corresponds to general experience with galvanic metal deposits. So it could be that all the WO_3 adheres at the surface. A small amount would adhere at the relatively smooth surface of a thin coating. Large amounts would be trapped in the very rough surface of a thick coating. Two findings, however, finally prove the homogeneous distribution:

(*i*) SEM micrographs of a cross section of the composite [26]. These reveal clearly a quite homogeneous distribution of the pigment.

(*ii*) SEM micrographs of the surface of anodically grown PPy/TiO_2 composits are shown in Fig. 8 for three c_Cs. The TiO_2 particles can be easily recognized, and a diameter of 0.5 μm can be deduced, in agreement with direct determination [27]. The surface density remains virtually constant. If the bulk concentration were negligible, and all TiO_2 material had accumulated at the surface due to the increase in surface roughness, a much stronger density would be seen at higher (average) loadings. The good proportionality in Fig. 5 would not be verified.

The medium particle size of 10 μm for WO_3 seems to be too large for the composite formation. Figure

9 presents the particle size distribution data for WO_3 in water or acetonitrile, after stirring and after ultra sonic treatment. Clearly, fractions of particle sizes extend down to the region well below 1 μm. From this it is concluded that agglomerates are present, which can be further dispersed. The SEM technique reveals that mainly agglomorates are present at the surface of the composite, but with a lower individual particle size, *cf.* [28]. The diameter of the primary particle seems to be in the order of 0.1 μm. This is not much larger than the primary particle size in the case of TiO_2, *cf.* Fig. 8 and [27], where the dispersability of the pigment was improved. It is interesting to note

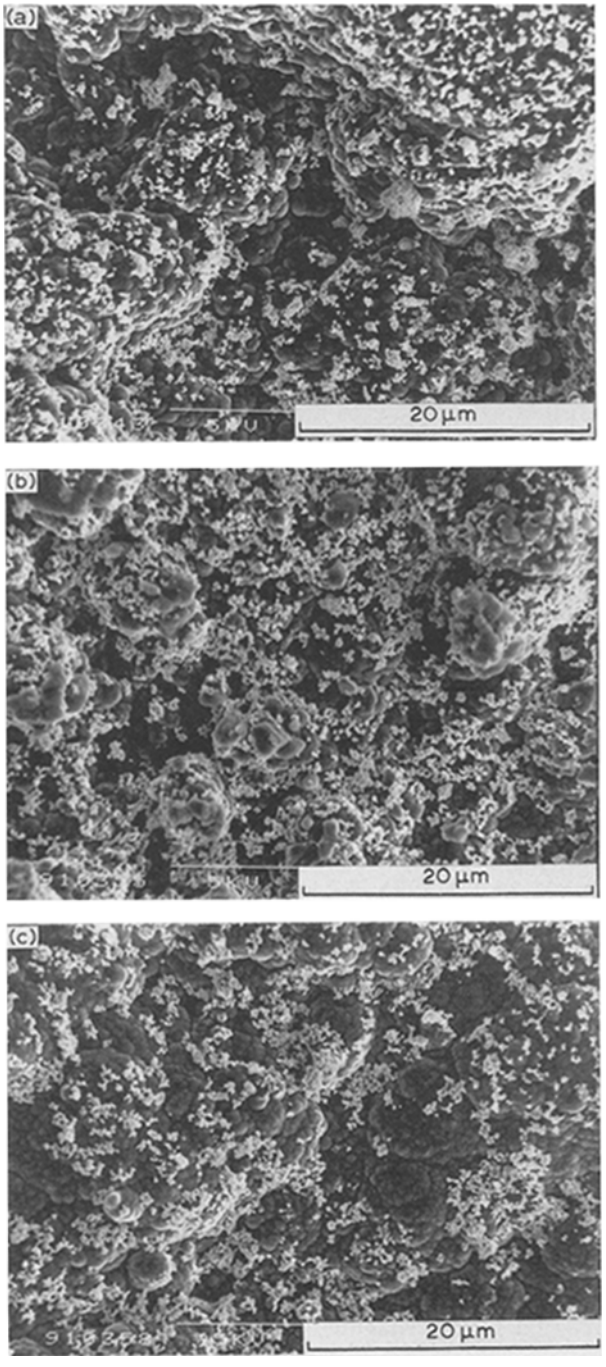

Fig. 8. SEM micrographs. Top views of electrodeposited PPy/TiO_2 codeposits of various thicknesses [27]. Electrolyte II (H_2O), base electrode stainless steel (Remanit^{TM}, Thyssen A.G.), polished with diamond 1 μm. Convection PL, $c_E = 30\,g\,TiO_2\,dm^{-3}$. (a) $d_n = 3\,\mu m$, (b) $d_n = 10\,\mu m$, and (c) $d_n = 30\,\mu m$.

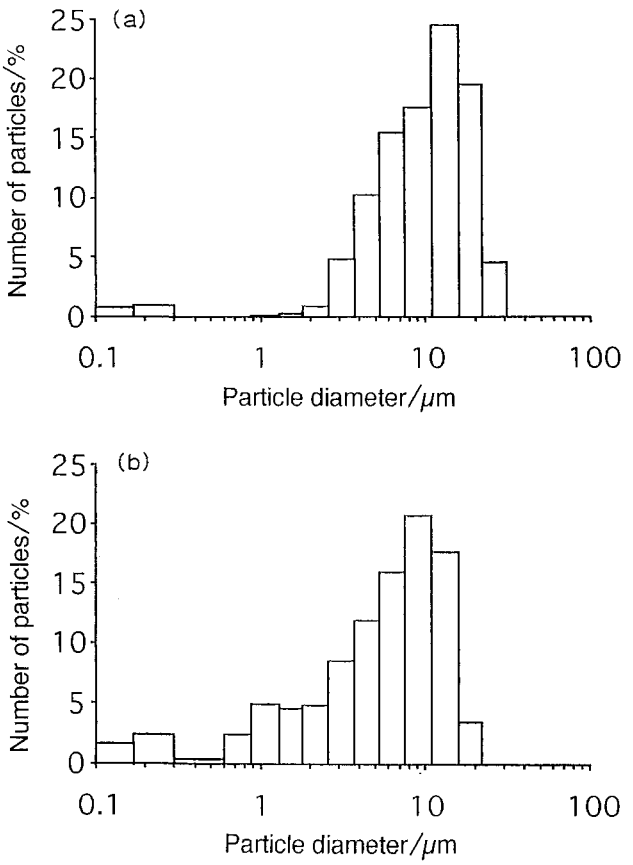

Fig. 9. Particle size distribution of WO_3 in aqueous 0.1 M $LiClO_4$. (a) stirred solution, (b) ultrasonic treatment.

that the present results demonstrate the possibility of selection of the codeposition conditions in favour of smaller particle sizes. It is to be expected, that the smaller particles are codeposited more easily. Very large particles are not incorporated permanently.

The experimental findings allow a comprehensive understanding of the codeposition mechanism. This parametric study forms the basis for the production of a wide variety of concentrations of WO_3 in PPy via variation of c_E, convection and current density. PPy/WO_3 materials and their characterization will be reported in a subsequent paper [28].

Acknowledgements

Financial support of this work by Deutsche Forschungsgemeinschaft (DFG) is gratefully acknowledged. We are indebted to Mr B. Pawlik, Shimadzu GmbH, Langenfeld, for analysing the particle size of the WO_3.

References

[1] A. Simons, *U.S. Patent 2 571 772* (1949).
[2] F. K. Sautter, *J. Electrochem. Soc.* **110** (1963) 557.
[3] G. R. Lakshminarayanan, E. S. Chen and F. K. Sautter, *ibid.* **122** (1975) 1589.
[4] J. P. Celis and J. R. Roos, *ibid.* **127** (1977) 1508.
[5] N. Nasuko, *Kinzoku-Hyomen-Gijutsu* **28** (1977) 534.
[6] C. White and J. Foster, *Trans. Instit. Metal Finish.* **59** (1981) 8.
[7] Y. Suzuki and O. Asai, *J. Electrochem. Soc.* **134** (1987) 1905.
[8] N. Guglielmi, *ibid.* **119** (1972) 1009.
[9] R. Babu, V. S. Muralidharan and K. I. Vasu, *Plating Surf. Finish.* (5) (1991) 126.

[10] P. W. Martin, *Metal Finish. J.* (11) (1965) 447.
[11] M. Metzger and H.-H. Tombrink, *Oberfläche/Surface* **14**(4) (1973) 67.
[12] M. N. Joshi and M. K. Totlani, Proceedings of the 2nd International Conference on Electroplating and Metal Finishing SAEST, Bombay (1981) p. 89.
[13] M. Fahnoe, *U.S. Patent 2 904 418* (1955).
[14] Daimler-Benz A.G., *U.S. Patent 2 999 798* (1955).
[15] H. R. Khan and Ch. J. Raub, *J. Less. Common Metals* **43** (1975) 49.
[16] J. Lessard and G. Belot *U.S. Patent 4 584 067* (1986).
[17] A. Anani, Z. Mao, S. Srinivasan and A. J. Appleby, *J. Electrochem. Soc.*.**21** (1991) 683.
[18] K. Naitoh, *Kinzoku-Hyomen-Gijutsu* **30**(4) (1979) 17.
[19] T. Hayashi, Galvanotechnique Meeting, DGO, Ulm (1989).
[20] P. W. Martin, *Metal Finish. J.* (10) (1965) 399.
[21] I. Rajagopal, *in* 'Surface Modification Technologies', (edited by T. S. Sudarshan), Marcel Dekker, New York (1989) pp. 1–47.
[22] H. Yoneyama, Y. Shoji and K. Kawai, *Chem. Lett.* (1989) 1067.
[23] K. Kawai, N. Mihara, S. Kuwabata and H. Yoneyama, *J. Electrochem. Soc.* **137** (1990) 1793.
[24] O. Ikeda and H. Yoneyama, *J. Electroanal. Chem.* **265** (1989) 323.
[25] M. Dufort, C. Levassort and L. Olmedo, *Synth. Metals* **41–43** (1991) 3063.
[26] N. Furukawa, T Saito and C. Iwakura, *Chem. Express* **5** (1990) 269.
[27] F. Beck, M. Dahlhaus and N. Zahedi, *Electrochim. Acta* **37** (1992) 1265.
[28] M. Dahlhaus and F. Beck, *J. Appl. Electrochem.*, submitted.
[29] A. F. Diaz, K. K. Kanizawa and G. P. Gardini, *J.C.S. Chem. Commum.* (1979) 854; A. F. Diaz, *Chem. Scripta* **17** (1981) 145.
[30] F. Beck and M. Oberst, *Makromol. Chem., Macromol. Symp.* **8** (1989) 97.
[31] G. Heydecke and F. Beck, *Carbon* **28** (1990) 301.
[32] G. Wünsch, 'Optische Analysenmethoden zur Bestimmung anorganischer Stoffe', Walter de Gruyter, Berlin (1976) p. 208.
[33] M. Oberst and F. Beck, *Angew. Chem.* **99** (1987) 1061; *Angew. Chem. Internat. Ed.* **26** (1987) 1031.
[34] F. Beck and M. Oberst, *J. Appl. Electrochem.* **22** (1992) 332.
[35] F. Beck, B. Wermeckes and M. Schirmeisen, *in* 'Electroorganic Synthesis – Festschrift for Manuel M. Baizer', (edited by R. D. Little and N. L. Weinberg) Marcel Dekker, New York (1991) p. 397.
[36] F. Beck and R. Michaelis, *J. Coat. Techn.* **64** (May 1992) 59.